Filter–and–Forward Beamforming for Multiple Multi–Antenna Relays

(Invited Paper)

Yang-wen Liang[†], Aissa Ikhlef[†], Wolfgang Gerstacker[††], and Robert Schober[†]
[†]Dept. of Elec. and Comp. Engineering, The University of British Columbia, E-mail: {yangl, aikhlef, rschober}@ece.ubc.ca
[††]Institute for Mobile Communications, University of Erlangen–Nürnberg, E-mail: gersta@LNT.de

Abstract—**In this paper, we investigate filter–and–forward beamforming (FF–BF) for relay networks employing single–carrier transmission over frequency–selective channels. In contrast to prior work, which concentrated on multiple single–antenna relay nodes, we consider networks employing multiple multi–antenna relay nodes. For the processing at the destination, we investigate two different cases: (1) A simple slicer without equalization and (2) a linear equalizer or a decision–feedback equalizer. For both cases, we optimize the FF–BF matrix filters at the relays for maximization of the signal–to–interference–plus–noise ratio (SINR) under a transmit power constraint, and for the first case we consider additionally optimization of the FF–BF matrix filters for minimization of the total transmit power under an SINR constraint. For the first case, we obtain closed–form solutions for the optimal finite impulse response (FIR) FF–BF matrix filters, whereas for the second case, we provide the optimal solution for infinite impulse response FF–BF matrix filters, and an efficient gradient algorithm for recursive calculation of near–optimal FIR FF–BF matrix filters. Our simulation results reveal that for a given total number of antennas in the network, a small number of multiple–antenna relays can achieve significant performance gains over a large number single–antenna relays.**

I. Introduction

Relaying is a promising technique to extend the range of wireless communication systems [1]. The two main relay protocols considered in the literature are amplify–and–forward (AF) and decode–and–forward (DF) relaying [1]. Thereby, AF relaying is generally believed to be less complex as the relays only perform a linear processing of the received signals, whereas the relays have to decode and re–encode the received signals in DF relaying. In AF relaying, beamforming (BF) across the relays is a simple yet efficient technique to improve capacity and reliability. BF for AF relays and frequency–flat channels has been extensively studied in the literature, cf. e.g. [2] and references therein.

Filter–and–forward (FF) relaying was first introduced in [3]. Similar to AF relaying, no decoding/re–encoding is needed at the relays and the relays merely perform linear processing of the received signals. More specifically, all the relay nodes are equipped with infinite impulse response (IIR) or finite impulse response (FIR) filters. In [3], a linear filtering transceiver design for relay networks with one relay node and frequency flat channels was considered. FF beamforming (FF–BF) for frequency–selective channels was proposed in [4] and [5]. In [4], only a simple slicer was employed at the destination requiring the FF–BF filters at the relays to equalize both the source–relay and the relay–destination channels. It was shown in [5] that substantial performance gains compared to the scheme in [4] are possible if simple linear equalization (LE) or decision–feedback equalization (DFE) is performed at the destination at the expense of an increase in complexity. Both [4] and [5] considered only single–antenna relay nodes. However, in certain applications such as mobile–to–mobile or sensor–to–sensor communication via a relay it is conceivable that both the source and the destination have small form factors and can accommodate only a single antenna but the relay may be able to accommodate multiple antennas. This is the main motivation for us to extend in this paper the results in [4] and [5] to multiple–antenna relays. As we will see, such an extension is not straightforward.

In this paper, we consider a cooperative network with one single–antenna source, one single–antenna destination, and multiple multi–antenna relay nodes. We assume single–carrier transmission and frequency–selective channels. The relays are equipped FF–BF matrix filters. The destination employs either a simple slicer without equalization or LE/DFE. In the former case, we optimize the FF–BF filters for maximization of the signal–to–interference–plus–noise ratio (SINR) under a transmit power constraint and for minimization of the transmit power under an SINR constraint, respectively. For both optimization criteria we find a closed–form solution for the optimal FIR FF–BF matrix filters at the relays. For the case of LE/DFE at the destination, we derive a closed–form expression for the frequency response of the optimal IIR FF–BF matrix filters, and a numerical algorithm with guaranteed convergence for optimization of the power allocation factor included in the expression. We also provide an efficient gradient algorithm for recursive calculation of near–optimal FIR FF–BF filters. Simulation results reveal that it is preferable to have one relay with multiple antennas rather than multiple relays with single antennas even if the total number of antennas is the same in both cases.

Organization: In Section II, the adopted system model is presented. The optimization of FIR FF–BF filters when the destination employs only a simple slicer is discussed in Section III, and the case where the destination employs LE/DFE is considered in Section IV. Simulation results are provided in Section V, and some conclusions are drawn in Section VI.

Notations: In this paper, $(\cdot)^T$, $(\cdot)^H$, $(\cdot)^*$, $\boldsymbol{I}_X$, $\boldsymbol{0}_X$, $\lambda_{\max}\{\cdot\}$, and $[\boldsymbol{X}]_{ij}$ denote transpose, Hermitian transpose, complex conjugate, the $X \times X$ identity matrix, the all–zero column vector of length X, the maximum eigenvalue of a matrix, and the element of matrix $\boldsymbol{X}$ in row i and column j, respectively. Moreover, $\mathcal{E}\{\cdot\}$, $\otimes$, $\oplus$, and $*$ denote expectation, the Kronecker product, the Kronecker sum, and discrete–time convolution, respectively. $\mathrm{diag}\{\boldsymbol{X}_1, \boldsymbol{X}_2, \ldots, \boldsymbol{X}_N\}$ denotes a block–diagonal matrix with matrices $\boldsymbol{X}_1, \boldsymbol{X}_2, \ldots, \boldsymbol{X}_N$ on the main diagonal. Furthermore, $X(f) \triangleq \mathcal{F}\{x[k]\} = \sum_{k=-\infty}^{\infty} x[k]e^{-j2\pi fk}$ is the Fourier transform of discrete–time signal $x[k]$.

II. System Model

We consider a relay network with one single–antenna source node, N_R multi–antenna relays, and one single–antenna des-

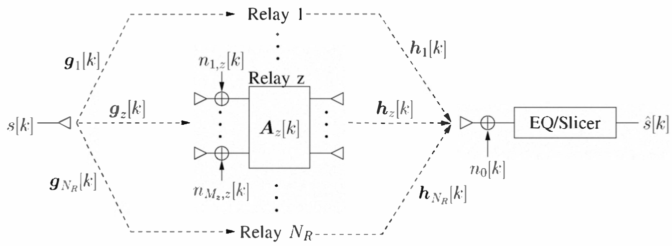

Fig. 1. Cooperative network with one single–antenna source, multiple multi–antenna relay nodes, and one single–antenna destination. EQ is the equalizer at the destination. $\hat{s}[k]$ are estimated symbols after the equalizer or slicer.

tination node. A block diagram of the discrete–time overall transmission system in equivalent complex baseband representation is shown in Fig. 1. As usual, transmission is organized in two intervals. In the first interval, the source node transmits a data packet which is received by the relays. In the second interval, the relays filter the received packet and forward it to the destination node. We assume that there is no direct link between the source and the destination node. At the destination, the data packets received during the second interval are processed and detected.

In Fig. 1, the discrete–time channel impulse responses (CIRs) between the source and the ith antenna of the zth relay, $g_{i,z}[k]$, $0 \leq k \leq L_g - 1$, and between antenna i of relay z and the destination, $h_{i,z}[k]$, $0 \leq k \leq L_h - 1$, contain the combined effects of transmit pulse shaping, the continuous–time channel, receive filtering, and sampling. Here, L_g and L_h denote the lengths of the source–relay and the relay–destination CIRs, respectively. Furthermore, we assume that relay z has M_z antennas and define $\boldsymbol{h}_z[k] \triangleq [h_{1,z}[k] \dots h_{M_z,z}[k]]^T$ and $\boldsymbol{g}_z[k] \triangleq [g_{1,z}[k] \dots g_{M_z,z}[k]]^T$.

In the following, we describe the processing performed at the relays and the destination in detail.

A. FF–BF at Relays

The signal received at the ith antenna, $i = 1, \dots, M_z$, of the zth relay, $z = 1, \dots, N_R$, during the first time interval is given by

$$y_{i,z}[k] = g_{i,z}[k] * s[k] + n_{i,z}[k] , \qquad (1)$$

where $s[k]$ are independent and identically distributed (i.i.d.) symbols taken from a scalar symbol alphabet $\mathcal{A}$ such as phase–shift keying (PSK) or quadrature amplitude modulation (QAM) with variance $\sigma_s^2 \triangleq \mathcal{E}\{|s[k]|^2\}$, and $n_{i,z}[k]$ denotes the additive white Gaussian noise (AWGN) at the ith receive antenna of the zth relay with variance $\sigma_n^2 \triangleq \mathcal{E}\{|n_{i,z}[k]|^2\}$.

The FF–BF matrix filter impulse response coefficients of relay z are denoted by $M_z \times M_z$ matrix $\boldsymbol{A}_z[k]$, $-q_l \leq k \leq q_u$, with elements $a_{ji,z}[k]$ on row j and column i. For IIR FF–BF matrix filters $q_l \to \infty$ and $q_u \to \infty$ and for FIR FF–BF filters $q_l = 0$ and $q_u = L_a - 1$, where L_a is the FIR FF–BF matrix filter length. The signal transmitted by the jth antenna, $j = 1, \dots, M_z$, of the zth relay, $z = 1, \dots, N_R$, during the second time interval can be expressed as

$$\begin{aligned} t_{j,z}[k] &= \sum_{i=1}^{M_z} a_{ji,z}[k] * y_{i,z}[k] \\ &= \sum_{i=1}^{M_z} a_{ji,z}[k] * g_{i,z}[k] * s[k] + \sum_{i=1}^{M_z} a_{ji,z}[k] * n_{i,z}[k] . \end{aligned} \qquad (2)$$

B. Processing at Destination

Since there is no direct link between the source and the destination, the signal received at the destination is given by

$$\begin{aligned} r[k] &= \sum_{z=1}^{N_R} \sum_{j=1}^{M_z} h_{j,z}[k] * t_{j,z}[k] + n_0[k] \\ &= h_{eq}[k] * s[k] + n[k] , \end{aligned} \qquad (3)$$

where $n_0[k]$ is AWGN with variance $\sigma_v^2 \triangleq \mathcal{E}\{|n_0[k]|^2\}$. The equivalent CIR $h_{eq}[k]$ between source and destination and the effective noise $n[k]$ are given by

$$h_{eq}[k] \triangleq \sum_{z=1}^{N_R} \sum_{j=1}^{M_z} h_{j,z}[k] * \sum_{i=1}^{M_z} a_{ji,z}[k] * g_{i,z}[k] , \qquad (4)$$

and

$$n[k] \triangleq \sum_{z=1}^{N_R} \sum_{j=1}^{M_z} h_{j,z}[k] * \sum_{i=1}^{M_z} a_{ji,z}[k] * n_{i,z}[k] + n_0[k] , \qquad (5)$$

respectively. Note that $n[k]$ is *colored* noise because of the filtering of $n_{i,z}[k]$ by $\boldsymbol{h}_z[k]$ and $\boldsymbol{A}_z[k]$. Eq. (3) shows that a cooperative relay network with FF–BF can be modeled as an equivalent single–input single–output (SISO) system. Therefore, as long as the destination knows the statistics of the colored noise $n[k]$, at the destination the same equalization, channel estimation, and channel tracking techniques as for point–to–point single–antenna transmission can be used. Here, we consider two cases: (1) The destination makes a decision based on $r[k]$ without equalization. (2) The destination first equalizes $r[k]$ using LE or DFE optimized under zero–forcing (ZF) and minimum mean–squared error (MMSE) criteria before making a decision [6]. The optimization of the corresponding FF–BF matrix filters will be discussed in Sections III and IV, respectively.

III. FF–BF WITHOUT EQUALIZATION

In this section, we consider the case where the destination node cannot afford an equalizer due to size and/or power limitations. Therefore, we assume that a simple slicer is employed at the destination throughout this section. In the following, we will optimize FIR FF–BF matrix filters for maximization of the SINR at the slicer output under a power constraint and for minimization of the transmit power under an SINR constraint, respectively.

The equivalent CIR $\mathbf{h}_{eq} \triangleq [h_{eq}[0]\ h_{eq}[1]\ \dots\ h_{eq}[L_a + L_g + L_h - 3]]^T$ between source and destination in Eq. (4) can be rewritten as

$$\mathbf{h}_{eq} = \sum_{z=1}^{N_R} \bar{\boldsymbol{H}}_z \bar{\boldsymbol{G}}_z \bar{\boldsymbol{a}}_z \triangleq \mathcal{H}\mathcal{G}\boldsymbol{a}, \qquad (6)$$

where $\mathcal{H} \triangleq [\bar{\boldsymbol{H}}_1\ \dots\ \bar{\boldsymbol{H}}_{N_R}]$, $\mathcal{G} \triangleq \mathrm{diag}\left\{\bar{\boldsymbol{G}}_1, \dots, \bar{\boldsymbol{G}}_{N_R}\right\}$, and $\boldsymbol{a} \triangleq [\bar{\boldsymbol{a}}_1^T\ \dots\ \bar{\boldsymbol{a}}_{N_R}^T]^T$. Here, $\mathcal{H}$ contains $(L_a + L_g + L_h - 2) \times (L_a + L_g - 1)M_z$ matrices $\bar{\boldsymbol{H}}_z \triangleq [\boldsymbol{H}_{1,z}\ \boldsymbol{H}_{2,z}\ \dots\ \boldsymbol{H}_{M_z,z}]$ with $(L_a + L_g + L_h - 2) \times (L_a + L_g - 1)$ column circular matrices $\boldsymbol{H}_{i,z}$, which have $[h_{i,z}[0]\ \dots\ h_{i,z}[L_h - 1]\ \boldsymbol{0}_{L_a+L_g-2}^T]^T$ in their first column. Furthermore, $\mathcal{G} \triangleq \mathrm{diag}\left\{\bar{\boldsymbol{G}}_1, \dots, \bar{\boldsymbol{G}}_{N_R}\right\}$ contains $(L_a + L_g - 1)M_z \times M_z^2 L_a$ matrices $\bar{\boldsymbol{G}}_z \triangleq \boldsymbol{I}_{M_z} \otimes [\boldsymbol{G}_{1,z}\ \dots\ \boldsymbol{G}_{M_z,z}]$ with $(L_a + L_g - 1) \times L_a$ column circular matrices $\boldsymbol{G}_{i,z}$ having vectors $[g_{i,z}[0]\ \dots\ g_{i,z}[L_g - 1]\ \boldsymbol{0}_{L_a-1}^T]^T$ in their first columns. Vector $\boldsymbol{a}$ contains $M_z^2 L_a \times 1$ vectors $\bar{\boldsymbol{a}}_z \triangleq [\boldsymbol{a}_{11,z}^T\ \boldsymbol{a}_{12,z}^T\ \dots\ \boldsymbol{a}_{1M_z,z}^T\ \boldsymbol{a}_{21,z}^T\ \dots\ \boldsymbol{a}_{M_z M_z,z}^T]^T$, which are comprised of vectors $\boldsymbol{a}_{ij,z} \triangleq [a_{ij,z}[0]\ a_{ij,z}[1]\ \dots\ a_{ij,z}[L_a - 1]]^T$.

Matrix $\mathcal{H}$ can be separated into one vector and one sub–matrix, i.e., $\mathcal{H} = [\bar{\boldsymbol{h}}_0\ \mathcal{H}_t^T]^T$, where $\mathcal{H}_t \triangleq [\mathcal{H}]_{ij}$, $2 \leq i \leq (L_a + L_g + L_h - 2)$, $1 \leq j \leq (L_a + L_g - 1)\sum_{z=1}^{N_R} M_z$, and vector $\bar{\boldsymbol{h}}_0$ has length $(L_a+L_g-1)\sum_{z=1}^{N_R} M_z$ and is given by $\bar{\boldsymbol{h}}_0 \triangleq [\boldsymbol{h}_{0,1}^T\ \boldsymbol{h}_{0,2}^T\ \dots\ \boldsymbol{h}_{0,N_R}^T]^T$ with $\boldsymbol{h}_{0,z} \triangleq [h_{1,z}[0]\ \boldsymbol{0}_{L_a+L_g-2}^T\ h_{2,z}[0]\ \boldsymbol{0}_{L_a+L_g-2}^T\ \dots\ h_{M_z,z}[0]\ \boldsymbol{0}_{L_a+L_g-2}^T]^T$. Therefore, the first term in (3) can be rewritten as

$$\begin{aligned} h_{eq}[k] * s[k] &= h_{eq}[0]s[k] + \sum_{l=1}^{L_a+L_g+L_h-3} h_{eq}[l]s[k-l] \\ &= \underbrace{\bar{\boldsymbol{h}}_0^T \mathcal{G}\boldsymbol{a}s[k]}_{\text{desired signal}} + \underbrace{\bar{\boldsymbol{s}}^T[k]\mathcal{H}_t\mathcal{G}\boldsymbol{a}}_{\text{ISI}} \end{aligned} \tag{7}$$

with $\bar{\boldsymbol{s}}[k] \triangleq [s[k-1]\ \dots\ s[k-(L_a+L_g+L_h-3)]]^T$. Therefore, the power of the desired signal and the intersymbol interference (ISI) can be obtained as

$$\mathcal{E}\left\{\left|\bar{\boldsymbol{h}}_0^T\mathcal{G}\boldsymbol{a}s[k]\right|^2\right\} = \sigma_s^2\boldsymbol{a}^H\mathcal{G}^H\bar{\boldsymbol{h}}_0^*\bar{\boldsymbol{h}}_0^T\mathcal{G}\boldsymbol{a} \tag{8}$$

and

$$\mathcal{E}\left\{\left|\bar{\boldsymbol{s}}^T[k]\mathcal{H}_t\mathcal{G}\boldsymbol{a}\right|^2\right\} = \sigma_s^2\boldsymbol{a}^H\mathcal{G}^H\mathcal{H}_t^H\mathcal{H}_t\mathcal{G}\boldsymbol{a}\,, \tag{9}$$

respectively. Similarly, $n[k]$ in (5) can be rewritten as

$$n[k] = \sum_{z=1}^{N_R}\bar{\boldsymbol{n}}_z[k]\breve{\boldsymbol{H}}_z\bar{\boldsymbol{a}}_z + n_0[k] \triangleq \mathcal{N}[k]\breve{\mathcal{H}}\boldsymbol{a} + n_0[k] \tag{10}$$

with length $\sum_{z=1}^{N_R}(L_a + L_h - 1)M_z$ row vector $\mathcal{N}[k] \triangleq [\bar{\boldsymbol{n}}_1[k]\ \dots\ \bar{\boldsymbol{n}}_{N_R}[k]]$ and $\sum_{z=1}^{N_R}(L_a+L_h-1)M_z \times \sum_{z=1}^{N_R} M_z^2 L_a$ matrix $\breve{\mathcal{H}} \triangleq \operatorname{diag}\left\{\breve{\boldsymbol{H}}_1,\ \dots,\ \breve{\boldsymbol{H}}_{N_R}\right\}$. Moreover, $\bar{\boldsymbol{n}}_z[k] \triangleq [\boldsymbol{n}_{1,z}[k]\ \dots\ \boldsymbol{n}_{M_z,z}[k]]$ with $\boldsymbol{n}_{i,z}[k] \triangleq [n_{i,z}[k]\ \dots\ n_{i,z}[k-(L_a+L_h-2)]]$, and $\breve{\boldsymbol{H}}_z \triangleq [\boldsymbol{I}_{M_z} \otimes \tilde{\boldsymbol{H}}_{1,z}\ \dots\ \boldsymbol{I}_{M_z} \otimes \tilde{\boldsymbol{H}}_{M_z,z}]$. $(L_a + L_h - 1) \times L_a$ column circular matrix $\tilde{\boldsymbol{H}}_{i,z}$ has vector $[h_{i,z}[0]\ \dots\ h_{i,z}[L_h-1]\ \boldsymbol{0}_{L_a-1}^T]^T$ in the first column. The noise power can be expressed as

$$\mathcal{E}\{|n[k]|^2\} = \sigma_n^2\boldsymbol{a}^H\breve{\mathcal{H}}^H\breve{\mathcal{H}}\boldsymbol{a} + \sigma_v^2\,. \tag{11}$$

From (8), (9), and (11), the SINR at the destination can be obtained as

$$\begin{aligned} \text{SINR}\,(\boldsymbol{a}) &= \frac{\mathcal{E}\left\{\left|\bar{\boldsymbol{h}}_0^T\mathcal{G}\boldsymbol{a}s[k]\right|^2\right\}}{\mathcal{E}\left\{\left|\bar{\boldsymbol{s}}^T[k]\mathcal{H}_t\mathcal{G}\boldsymbol{a}\right|^2\right\} + \mathcal{E}\{|n[k]|^2\}} \\ &= \frac{\boldsymbol{a}^H\boldsymbol{W}_1\boldsymbol{a}}{\boldsymbol{a}^H\boldsymbol{W}_2\boldsymbol{a} + \boldsymbol{a}^H\boldsymbol{W}_3\boldsymbol{a} + 1} \end{aligned} \tag{12}$$

with $\boldsymbol{W}_1 \triangleq \sigma_s^2\mathcal{G}^H\bar{\boldsymbol{h}}_0^*\bar{\boldsymbol{h}}_0^T\mathcal{G}/\sigma_v^2$, $\boldsymbol{W}_2 \triangleq \sigma_s^2\mathcal{G}^H\mathcal{H}_t^H\mathcal{H}_t\mathcal{G}/\sigma_v^2$, and $\boldsymbol{W}_3 \triangleq \sigma_n^2\breve{\mathcal{H}}^H\breve{\mathcal{H}}/\sigma_v^2$.

From (2), the total transmit power, P_R, of the relays can be obtained as

$$P_R = \sum_{z=1}^{N_R}\sum_{j=1}^{M_z}\mathcal{E}\left\{|t_{j,z}[k]|^2\right\} = \boldsymbol{a}^H\boldsymbol{D}\boldsymbol{a}\,, \tag{13}$$

with $\boldsymbol{D} \triangleq \sigma_s^2\mathcal{G}^H\mathcal{G} + \sigma_n^2\boldsymbol{I}_{L_a\sum_{z=1}^{N_R} M_z^2}$.

In the following, we will formulate various FF–BF filter optimization problems based on (12) and (13).

A. SINR Maximization Under Relay Power Constraint

First, we consider the optimization of the FF–BF matrix filters for maximization of the SINR subject to maximum relay power P. Accordingly, the optimization problem can be formulated as

$$\max_{\boldsymbol{a}} \quad \text{SINR}\,(\boldsymbol{a}) \tag{14a}$$

$$s.t. \quad \boldsymbol{a}^H\boldsymbol{D}\boldsymbol{a} \leq P\,. \tag{14b}$$

By letting $\boldsymbol{w} \triangleq \boldsymbol{D}^{1/2}\boldsymbol{a}$, where $\boldsymbol{D}^{1/2}$ is the Cholesky decomposition of $\boldsymbol{D}$, the optimization problem in (14) can be reformulated as a generalized eigenvalue problem. The optimum $\boldsymbol{w}$ can be obtained as

$$\begin{aligned} \boldsymbol{w}_{\text{opt}} &= \sqrt{P}\boldsymbol{u}\left\{\boldsymbol{Q}_1^{-1}\boldsymbol{D}^{-H/2}\boldsymbol{W}_1\boldsymbol{D}^{-1/2}\right\} \\ &= \frac{\sqrt{P}\boldsymbol{Q}_1^{-1}\boldsymbol{D}^{-H/2}\mathcal{G}^H\bar{\boldsymbol{h}}_0^*}{\sqrt{\bar{\boldsymbol{h}}_0^T\mathcal{G}\boldsymbol{D}^{-1/2}\boldsymbol{Q}_1^{-2}\boldsymbol{D}^{-H/2}\mathcal{G}^H\bar{\boldsymbol{h}}_0^*}}\,, \end{aligned} \tag{15}$$

where $\boldsymbol{Q}_1 \triangleq \boldsymbol{D}^{-H/2}\left(\boldsymbol{W}_2 + \boldsymbol{W}_3\right)\boldsymbol{D}^{-1/2} + \frac{1}{P}\boldsymbol{I}_{L_a\sum_{z=1}^{N_R} M_z^2}$ and $\boldsymbol{u}\{\boldsymbol{X}\}$ is the principle eigenvector of matrix $\boldsymbol{X}$. Therefore, the maximum SINR can be obtained as

$$\text{SINR}_{\max} = \frac{\sigma_s^2}{\sigma_v^2}\bar{\boldsymbol{h}}_0^T\mathcal{G}\left(\boldsymbol{W}_2 + \boldsymbol{W}_3 + \frac{1}{P}\boldsymbol{D}\right)^{-1}\mathcal{G}^H\bar{\boldsymbol{h}}_0^*\,, \tag{16}$$

and the corresponding optimum FF–BF matrix filter in vector form is given as

$$\boldsymbol{a}_{\text{opt}} = \frac{\sqrt{P}\left(\boldsymbol{W}_2 + \boldsymbol{W}_3 + \frac{1}{P}\boldsymbol{D}\right)^{-1}\mathcal{G}^H\bar{\boldsymbol{h}}_0^*}{\sqrt{\bar{\boldsymbol{h}}_0^T\mathcal{G}\boldsymbol{D}^{-1/2}\boldsymbol{Q}_1^{-2}\boldsymbol{D}^{-H/2}\mathcal{G}^H\bar{\boldsymbol{h}}_0^*}}\,. \tag{17}$$

B. Relay Power Minimization Under SINR Constraint

Here, we optimize the FF–BF matrix filters for minimization of the relay transmit power, $P_R(\boldsymbol{a})$, subject to an SINR constraint. The optimization problem can be formulated as

$$\min_{\boldsymbol{a}} \quad P_R(\boldsymbol{a}) = \boldsymbol{a}^H\boldsymbol{D}\boldsymbol{a} \tag{18a}$$

$$s.t. \quad \frac{\boldsymbol{a}^H\boldsymbol{W}_1\boldsymbol{a}}{\boldsymbol{a}^H\boldsymbol{W}_2\boldsymbol{a} + \boldsymbol{a}^H\boldsymbol{W}_3\boldsymbol{a} + 1} \geq \gamma\,, \tag{18b}$$

where γ is the minimal required SINR at the destination. We let $\boldsymbol{w} = \boldsymbol{D}^{1/2}\boldsymbol{a}$ again and note that the above problem is infeasible when $\boldsymbol{Q}_2 \triangleq \boldsymbol{D}^{-H/2}\left(\boldsymbol{W}_1 - \gamma\boldsymbol{W}_2 - \gamma\boldsymbol{W}_3\right)\boldsymbol{D}^{-1/2}$, is negative semidefinite. If the problem is feasible, the optimum FF–BF matrix filter can be obtained as

$$\boldsymbol{a}_{\text{opt}} = \left(\frac{\gamma}{\lambda_{\max}\{\boldsymbol{Q}_2\}}\right)^{1/2}\boldsymbol{D}^{-1/2}\boldsymbol{u}\{\boldsymbol{Q}_2\} \tag{19}$$

and the corresponding minimum relay power is

$$P_{\min} = \frac{\gamma}{\lambda_{\max}\{\boldsymbol{Q}_2\}}\,. \tag{20}$$

C. SINR Maximization Under Source–Relay Power Constraint

Compared to the case with separate power constraints for the source and the relays, which was considered in Section III-A, additional performance gains are possible with a joint source–relay transmit power constraint. The corresponding optimization problem can be formulated as

$$\max_{\boldsymbol{a},\,\sigma_s^2} \quad \frac{\boldsymbol{a}^H\boldsymbol{W}_1\boldsymbol{a}}{\boldsymbol{a}^H\boldsymbol{W}_2\boldsymbol{a} + \boldsymbol{a}^H\boldsymbol{W}_3\boldsymbol{a} + 1} \tag{21a}$$

$$s.t. \quad \boldsymbol{a}^H\boldsymbol{D}\boldsymbol{a} + \sigma_s^2 \leq P \tag{21b}$$

The optimal solution can be found with a divide–and–conquer method. In particular, if we assume that σ_s^2 is fixed, problem (21) is identical to problem (14). The optimum FF–BF matrix filter is obtained as

$$\boldsymbol{a}_{\mathrm{opt}} = \frac{\sqrt{P-\sigma_s^2}\left(\boldsymbol{W}_2(\sigma_s^2)+\boldsymbol{W}_3+\frac{\boldsymbol{D}(\sigma_s^2)}{P-\sigma_s^2}\right)^{-1}\mathcal{G}^H\bar{\boldsymbol{h}}_0^*}{\sqrt{\bar{\boldsymbol{h}}_0^T\mathcal{G}\boldsymbol{D}^{-1/2}(\sigma_s^2)\boldsymbol{Q}_1^{-2}(\sigma_s^2)\boldsymbol{D}^{-H/2}(\sigma_s^2)\mathcal{G}^H\bar{\boldsymbol{h}}_0^*}}, \quad (22)$$

and the corresponding maximum SINR is given by

$$\begin{aligned}&\mathrm{SINR}_{\max}(\sigma_s^2)\\ &= \frac{\sigma_s^2}{\sigma_v^2}\bar{\boldsymbol{h}}_0^T\mathcal{G}\left(\boldsymbol{W}_2(\sigma_s^2)+\boldsymbol{W}_3+\frac{\boldsymbol{D}(\sigma_s^2)}{P-\sigma_s^2}\right)^{-1}\mathcal{G}^H\bar{\boldsymbol{h}}_0^* \quad (23)\end{aligned}$$

where

$$\begin{aligned}\boldsymbol{Q}_1(\sigma_s^2) &\triangleq \boldsymbol{D}^{-H/2}(\sigma_s^2)\left(\boldsymbol{W}_2(\sigma_s^2)+\boldsymbol{W}_3\right)\boldsymbol{D}^{-1/2}(\sigma_s^2)\\ &\quad+\frac{1}{P-\sigma_s^2}\boldsymbol{I}_{L_a\sum_{z=1}^{N_R}M_z^2}. \quad (24)\end{aligned}$$

Note that $\boldsymbol{D}$, $\boldsymbol{W}_1$, and $\boldsymbol{W}_2$ defined earlier depend now all on σ_s^2. The remaining problem is to find the optimal σ_s^2 such that $\mathrm{SINR}_{\max}(\sigma_s^2)$ is maximized, i.e.

$$\max_{\sigma_s^2,\,0\le\sigma_s^2\le P} \quad \mathrm{SINR}_{\max}(\sigma_s^2). \quad (25)$$

Problem (25) can be easily solved by a grid search or other numerical methods given in [7].

D. Source–Relay Power Minimization Under SINR Constraint

In this case, the goal is to minimize the joint source–relay transmit power subject to a destination SINR constraint. The optimization problem can be formulated as

$$\min_{\boldsymbol{a},\,\sigma_s^2} \quad \boldsymbol{a}^H\boldsymbol{D}\boldsymbol{a}+\sigma_s^2 \quad (26a)$$

$$s.t. \quad \frac{\boldsymbol{a}^H\boldsymbol{W}_1\boldsymbol{a}}{\boldsymbol{a}^H\boldsymbol{W}_2\boldsymbol{a}+\boldsymbol{a}^H\boldsymbol{W}_3\boldsymbol{a}+1}\ge\gamma \quad (26b)$$

Again, we assume that σ_s^2 is fixed, and the resulting problem is identical to problem (18). If the problem is feasible, the optimum FF–BF matrix filter is given by

$$\boldsymbol{a}_{\mathrm{opt}} = \left(\frac{\gamma}{\lambda_{\max}\{\boldsymbol{Q}_2(\sigma_s^2)\}}\right)^{1/2}\boldsymbol{D}^{-1/2}(\sigma_s^2)\boldsymbol{u}\{\boldsymbol{Q}_2(\sigma_s^2)\}, \quad (27)$$

and the corresponding minimum joint source–relay transmit power is

$$P_{\min} = \frac{\gamma}{\lambda_{\max}\{\boldsymbol{Q}_2(\sigma_s^2)\}}+\sigma_s^2 \quad (28)$$

with $\boldsymbol{Q}_2(\sigma_s^2) \triangleq \boldsymbol{D}^{-H/2}(\sigma_s^2)\left(\boldsymbol{W}_1(\sigma_s^2)-\gamma\boldsymbol{W}_2(\sigma_s^2)-\gamma\boldsymbol{W}_3\right) \times\boldsymbol{D}^{-1/2}(\sigma_s^2)$. The remaining optimization problem is

$$\min_{\sigma_s^2} \quad \frac{\gamma}{\lambda_{\max}\{\boldsymbol{Q}_2(\sigma_s^2)\}}+\sigma_s^2 \quad (29a)$$

$$s.t. \quad \lambda_{\max}\{\boldsymbol{Q}_2(\sigma_s^2)\}>0. \quad (29b)$$

$\sigma_s^2=0$ has been ignored in problem (29) due to the fact that (29b) is satisfied only if $\sigma_s^2>0$. Problem (29) can be easily solved by numerical methods given in [7].

We note that the results for multi–antenna relays in Sections III-A and III-B are extensions of the results for single–antenna relays given in [4]. Joint source–relay power constraints as considered in Sections III-C and III-D were not discussed in [4].

IV. FF–BF with Equalization

Throughout this section we assume that the destination node employs LE or DFE with IIR equalization filters. In a practical implementation, FIR equalization filters are used, of course. However, sufficiently long FIR filters will approach the performance of IIR filters arbitrarily close. Assuming IIR equalization filters has the advantage that relatively simple and elegant expressions for the SINR at the equalizer output exist [8], [9].

A. Optimal IIR FF–BF with Equalization

In order to exploit the SINR expressions in [8], [9], we first have to whiten the noise impairing the signal received at the destination. The power spectral density of $n[k]$ in (5) can be obtained as

$$\begin{aligned}\Phi_n(f) &= \sigma_n^2\sum_{z=1}^{N_R}\sum_{i=1}^{M_z}\left|\sum_{j=1}^{M_z}H_{j,z}(f)A_{ji,z}(f)\right|^2+\sigma_v^2\\ &= \sigma_n^2\boldsymbol{a}^H(f)\boldsymbol{\Gamma}(f)\boldsymbol{a}(f)+\sigma_v^2 \quad (30)\end{aligned}$$

with $\sum_{z=1}^{N_R}M_z^2 \times \sum_{z=1}^{N_R}M_z^2$ square matrix $\boldsymbol{\Gamma}(f) \triangleq \mathrm{diag}\{\boldsymbol{\Gamma}_1(f),\,\ldots,\,\boldsymbol{\Gamma}_{N_R}(f)\}$, where $\boldsymbol{\Gamma}_z(f) \triangleq \left(\boldsymbol{h}_z^*(f)\boldsymbol{h}_z^T(f)\right)\otimes\boldsymbol{I}_{M_z}$ and $\boldsymbol{h}_z(f) \triangleq [H_{1,z}(f),\,\ldots,\,H_{M_z,z}(f)]^T$. The frequency response of the relay–destination channel corresponding to the jth antenna of the zth relay is given by $H_{j,z}(f)\triangleq\mathcal{F}\{h_{j,z}[k]\}$. The frequency responses of the FF–BF matrix filters are collected in vector $\boldsymbol{a}(f) \triangleq [\boldsymbol{a}_1^T(f)\,\ldots\,\boldsymbol{a}_{N_R}^T(f)]^T$ with $\boldsymbol{a}_z(f) \triangleq [A_{11,z}(f)\; A_{12,z}(f)\,\ldots\,A_{M_zM_z,z}(f)]^T$, where $A_{ji,z}(f)\triangleq\mathcal{F}\{a_{ji,z}[k]\}$ denotes the frequency response of the FF–BF matrix filter at relay z corresponding to the ith receive antenna and the jth transmit antenna. The whitening filter $W(f)$ for $n[k]$ can be easily obtained as

$$\begin{aligned}W(f) &= \left(\sigma_n^2\sum_{z=1}^{N_R}\sum_{i=1}^{M_z}\left|\sum_{j=1}^{M_z}H_{j,z}(f)A_{ji,z}(f)\right|^2+\sigma_v^2\right)^{-1/2}\\ &= \left(\sigma_n^2\boldsymbol{a}^H(f)\boldsymbol{\Gamma}(f)\boldsymbol{a}(f)+\sigma_v^2\right)^{-1/2}, \quad (31)\end{aligned}$$

and we denote the output of the whitening filter by $r'[k]$. Taking into account the whitening, the frequency response of the equivalent overall channel can be obtained as

$$\begin{aligned}&H'_{eq}(f)\triangleq W(f)\mathcal{F}\{h_{eq}[k]\}\\ &\quad=\left(\sigma_n^2\boldsymbol{a}^H(f)\boldsymbol{\Gamma}(f)\boldsymbol{a}(f)+\sigma_v^2\right)^{-1/2}\boldsymbol{q}^T(f)\boldsymbol{a}(f) \quad (32)\end{aligned}$$

with $\boldsymbol{q}(f)\triangleq[\boldsymbol{q}_1^T(f)\,\ldots\,\boldsymbol{q}_{N_R}^T(f)]^T$, $\boldsymbol{q}_z(f)\triangleq\boldsymbol{h}_z(f)\otimes\boldsymbol{g}_z(f)$, $\boldsymbol{g}_z(f)\triangleq[G_{1,z}(f)\;G_{2,z}(f)\,\ldots\,G_{M_z,z}(f)]^T$, $G_{i,z}(f)\triangleq\mathcal{F}\{g_{i,z}[k]\}$, and $\boldsymbol{h}_z(f)\triangleq[H_{1,z}(f)\;H_{2,z}(f)\,\ldots\,H_{M_z,z}(f)]^T$. The power spectral density of the noise component, $n'[k]$, of $r'[k]$ is $\Phi_{n'}(f)=1$.

In the remainder of this section, we formulate and solve the IIR FF–BF filter optimization problems for LE, DFE, and an idealized matched filter (MF) receiver in a unified manner. We can express the SINRs at the outputs of a decision feedback and a linear equalizer as [8]–[9]

$$\begin{aligned}&\mathrm{SINR}_{\mathrm{DFE}}(\boldsymbol{a}(f))\\ &\quad=\sigma_s^2\exp\left\{\int_{-1/2}^{1/2}\ln\left(|H'_{eq}(f)|^2+\xi\right)\,\mathrm{d}f\right\}-\chi \quad (33)\end{aligned}$$

and

$$\mathrm{SINR_{LE}}(\boldsymbol{a}(f)) = \sigma_s^2 \left(\int_{-1/2}^{1/2} \left(|H'_{eq}(f)|^2 + \xi \right)^{-1} \mathrm{d}f \right)^{-1} - \chi, \quad (34)$$

respectively. In (33) and (34), we have $\chi = 0$, $\xi = 0$ and $\chi = 1$, $\xi = 1/\sigma_s^2$ if the equalization filters are optimized based on a ZF and an MMSE criterion, respectively. Similarly, if only a single, isolated symbol $s[k]$ is transmitted, the SINR at the output of an MF is given by [6]

$$\mathrm{SINR_{MF}}(\boldsymbol{a}(f)) = \sigma_s^2 \int_{-1/2}^{1/2} |H'_{eq}(f)|^2 \, \mathrm{d}f. \quad (35)$$

In this section, our goal is to optimize the FF–BF matrix filters for maximization of the SINRs at the output of the considered equalizers. To make the problem well defined, we constrain the relay transmit power, P_R, which is given by

$$\begin{aligned} P_R &= \sum_{z=1}^{N_R} \sum_{j=1}^{M_z} \int_{-1/2}^{1/2} \Phi_{t_{j,z}}(f) \mathrm{d}f \\ &= \int_{-1/2}^{1/2} \boldsymbol{a}^H(f) \hat{\boldsymbol{D}}(f) \boldsymbol{a}(f) \mathrm{d}f \leq P \quad (36) \end{aligned}$$

where $\Phi_{t_{j,z}}(f) \triangleq \sigma_s^2 |\sum_{i=1}^{M_z} A_{ji,z}(f) G_{i,z}(f)|^2 + \sigma_n^2 \sum_{i=1}^{M_z} |A_{ji,z}(f)|^2$, $z = 1, \ldots, N_R$, $j = 1, \ldots, M_z$, is the power spectral density of the transmit signal $t_{j,z}[k]$ at the jth antenna of the zth relay, $\hat{\boldsymbol{D}}(f) \triangleq \sigma_s^2 \boldsymbol{G}^H(f) \boldsymbol{G}(f) + \sigma_n^2 \boldsymbol{I}_{\sum_{z=1}^{N_R} M_z^2}$, $\boldsymbol{G}(f) \triangleq \mathrm{diag}\{\boldsymbol{G}_1(f), \ldots, \boldsymbol{G}_{N_R}(f)\}$, and $\boldsymbol{G}_z(f) \triangleq \boldsymbol{I}_{M_z} \otimes \boldsymbol{g}_z^T(f)$.

Formally, the IIR FF–BF filter optimization problem can now be stated as

$$\max_{\boldsymbol{a}(f)} \quad \mathrm{SINR_X}(\boldsymbol{a}(f)) \quad (37a)$$

$$\text{s.t.} \quad \int_{-1/2}^{1/2} \boldsymbol{a}^H(f) \hat{\boldsymbol{D}}(f) \boldsymbol{a}(f) \, \mathrm{d}f \leq P, \quad (37b)$$

where P denotes the maximum relay transmit power, and X = DFE, X = LE, and X = MF for DFE, LE, and an MF receiver, respectively. Problem (37) is formally similar to the FF–BF filter optimization problem for single–antenna relays considered in [5]. The main difference is the definition of the involved matrices. Thus, the results given in [5] can also be exploited for solving (37). In particular, the optimum $\boldsymbol{a}(f)$ is given by

$$\boldsymbol{a}_{\mathrm{opt}}(f) = \sqrt{p(f)} c(f) \Big(\sigma_n^2 p(f) \boldsymbol{\Gamma}(f) + \sigma_v^2 \hat{\boldsymbol{D}}(f) \Big)^{-1} \boldsymbol{q}^*(f), \quad (38)$$

where $p(f)$ is the power allocation for frequency f and

$$c(f) \triangleq \left(\boldsymbol{q}^T(f) \hat{\boldsymbol{D}}^{-1/2}(f) \boldsymbol{X}^{-2}(f) \hat{\boldsymbol{D}}^{-H/2}(f) \boldsymbol{q}^*(f) \right)^{-1/2} \quad (39)$$

with $\boldsymbol{X}(f) \triangleq p(f) \sigma_n^2 \hat{\boldsymbol{D}}^{-H/2}(f) \boldsymbol{\Gamma}(f) \hat{\boldsymbol{D}}^{-1/2}(f) + \sigma_v^2 \boldsymbol{I}_{\sum_{z=1}^{N_R} M_z^2}$. From (38), the optimum individual FF–BF filter of relay z, $\boldsymbol{a}_z^{\mathrm{opt}}(f)$, can be simplified as

$$\begin{aligned} \boldsymbol{a}_z^{\mathrm{opt}}(f) =& \sqrt{p(f)} c(f) \Big(\sigma_n^2 p(f) \boldsymbol{\Gamma}_z(f) + \sigma_v^2 \sigma_s^2 \boldsymbol{G}_z^H(f) \boldsymbol{G}_z(f) \\ &+ \sigma_n^2 \sigma_v^2 \boldsymbol{I}_{M_z^2} \Big)^{-1} \boldsymbol{q}_z^*(f) \\ =& \sqrt{p(f)} c(f) \Big(\sigma_n^2 p(f) \left[\boldsymbol{h}_z^*(f) \boldsymbol{h}_z^T(f) \right] \\ &\oplus \left[\sigma_v^2 \sigma_s^2 \boldsymbol{g}_z^*(f) \boldsymbol{g}_z^T(f) + \sigma_n^2 \sigma_v^2 \boldsymbol{I}_{M_z} \right] \Big)^{-1} \\ &\times \left(\boldsymbol{h}_z^*(f) \otimes \boldsymbol{g}_z^*(f) \right) \quad (40) \\ =& \frac{\sqrt{p(f)} c(f) \left(\boldsymbol{h}_z^*(f) \otimes \boldsymbol{g}_z^*(f) \right)}{\sigma_n^2 p(f) \|\boldsymbol{h}_z(f)\|^2 + \sigma_v^2 \sigma_s^2 \|\boldsymbol{g}_z(f)\|^2 + \sigma_n^2 \sigma_v^2}. \quad (41) \end{aligned}$$

The transformation from (40) to (41) is accomplished by exploiting the relation [10]

$$(\boldsymbol{M} \oplus \boldsymbol{N})^{-1} = \sum_{i=1}^{N} \sum_{j=1}^{N} \frac{(\boldsymbol{m}_i \otimes \boldsymbol{n}_j)(\bar{\boldsymbol{m}}_i \otimes \bar{\boldsymbol{n}}_j)^H}{\lambda_i(\boldsymbol{M}) + \lambda_j(\boldsymbol{N})}, \quad (42)$$

where $\boldsymbol{m}_i$, $\boldsymbol{n}_i$, $\bar{\boldsymbol{m}}_i$, and $\bar{\boldsymbol{n}}_i$ denote the eigenvectors of $N \times N$ matrices $\boldsymbol{M}$, $\boldsymbol{N}$, $\boldsymbol{M}^H$, and $\boldsymbol{N}^H$, respectively. Therefore, the optimum beamforming matrix filter $A_z^{\mathrm{opt}}(f)$ of relay z is obtained as

$$A_z^{\mathrm{opt}}(f) = \frac{\sqrt{p(f)} c(f) \boldsymbol{h}_z^*(f) \boldsymbol{g}_z^H(f)}{\sigma_n^2 p(f) \|\boldsymbol{h}_z(f)\|^2 + \sigma_v^2 \sigma_s^2 \|\boldsymbol{g}_z(f)\|^2 + \sigma_n^2 \sigma_v^2}. \quad (43)$$

Eq. (43) reveals that the optimal IIR FF–BF matrix filters for all considered receiver structures can be interpreted as the concatenation of a filter matched to the source–relay and the relay–destination link with frequency response $\boldsymbol{h}_z^*(f) \boldsymbol{g}_z^H(f)$ and a second filter whose frequency response $\sqrt{p(f)} c(f) / (\sigma_n^2 p(f) \|\boldsymbol{h}_z(f)\|^2 + \sigma_v^2 \|\boldsymbol{g}_z(f)\|^2 + \sigma_n^2 \sigma_v^2)$ depends on the power allocation, and thus on the particular equalizer used at the destination. The remaining power allocation problem is given by

$$\max_{p(f)} \quad \mathrm{SINR}_X(\boldsymbol{a}_{\mathrm{opt}}(f)) \quad (44a)$$

$$s.t. \quad \int_{-1/2}^{1/2} p(f) \, \mathrm{d}f \leq P, \quad (44b)$$

where the $|H'_{eq}(f)|^2$ in $\mathrm{SINR}_X(\boldsymbol{a}_{\mathrm{opt}}(f))$, cf. (33)–(35), becomes

$$\left| H'_{eq}(f) \right|^2 = p(f) \boldsymbol{q}^T(f) \Big(p(f) \sigma_n^2 \boldsymbol{\Gamma}(f) + \sigma_v^2 \hat{\boldsymbol{D}}(f) \Big)^{-1} \boldsymbol{q}^*(f), \quad (45)$$

and X = DFE, X = LE, and X = MF for DFE, LE, and an MF at the receiver, respectively. Problem (44) is a convex optimization problem, and an efficient numerical algorithm for its solution is given in [5, Table 1].

B. Optimal FIR FF–BF with Equalization

In practice, it is not possible to implement the IIR FF–BF filters discussed in the previous section since they would require the feedback of an infinite number of filter coefficients from the destination to the relays. However, the performance achievable with these IIR FF–BF filters provides a useful upper bound for the FIR FF–BF filters considered in this section. In particular, the performance of the IIR solution can be used for optimizing the FIR BF–FF length to achieve a desired trade–off between the amount of feedback and performance. We note that although FIR FF–BF filters are considered in this section, the equalizers at the destination are still assumed to employ IIR filters.

With FIR FF–BF filters of length L_a at the relays, the length of the equivalent CIR $h_{\mathrm{eq}}[k]$ (4) is given by $L_{\mathrm{eq}} = L_a + L_g + L_h - 2$. In this case, the Fourier transform of $h_{\mathrm{eq}}[k]$ can be expressed as

$$H_{\mathrm{eq}}(f) = \boldsymbol{d}^H(f)\mathcal{H}\mathcal{G}\boldsymbol{a} \tag{46}$$

with $\boldsymbol{d}(f) \triangleq [1\ e^{j2\pi f}\ \ldots\ e^{j2\pi f(L_{\mathrm{eq}}-1)}]^T$. FIR FF–BF coefficient vector $\boldsymbol{a}$, $\mathcal{H}$, and $\mathcal{G}$ are defined in Section III after (6), respectively.

The noise whitening filter in the FIR case is given by

$$W(f) = \left(\sigma_n^2 \boldsymbol{a}^H \bar{\boldsymbol{\Gamma}}(f)\boldsymbol{a} + \sigma_v^2\right)^{-1/2} \tag{47}$$

with $\sum_{z=1}^{N_R} M_z^2 L_a \times \sum_{z=1}^{N_R} M_z^2 L_a$ block diagonal matrix $\bar{\boldsymbol{\Gamma}}(f) \triangleq \mathrm{diag}\left\{\bar{\boldsymbol{\Gamma}}_1(f), \ldots, \bar{\boldsymbol{\Gamma}}_{N_R}(f)\right\}$ of rank $\sum_{z=1}^{N_R} M_z$, where $\bar{\boldsymbol{\Gamma}}_z(f) \triangleq \breve{\boldsymbol{H}}_z^H \left(\boldsymbol{I}_{M_z} \otimes \bar{\boldsymbol{d}}(f)\right)\left(\boldsymbol{I}_{M_z} \otimes \bar{\boldsymbol{d}}(f)\right)^H \breve{\boldsymbol{H}}_z$ is an $M_z^2 L_a \times M_z^2 L_a$ matrix of rank M_z. $\breve{\boldsymbol{H}}_z$ is defined after (10), and $\bar{\boldsymbol{d}}(f) \triangleq [1\ e^{j2\pi f}\ \ldots\ e^{j2\pi f(L_h+L_a-2)}]^T$. Therefore, after noise whitening, the frequency response of the overall channel is

$$H'_{\mathrm{eq}}(f) = \boldsymbol{d}^H(f)\mathcal{H}\mathcal{G}\boldsymbol{a}\left(\sigma_n^2 \boldsymbol{a}^H \bar{\boldsymbol{\Gamma}}(f)\boldsymbol{a} + \sigma_v^2\right)^{-1/2}. \tag{48}$$

Replacing $H'_{\mathrm{eq}}(f)$ now in the SINR expressions in (33)–(35) by $H'_{\mathrm{eq}}(f)$ given in (48), we obtain the SINRs $\mathrm{SINR}_{\mathrm{X}}(\boldsymbol{a})$, where X = DFE, X = LE, and X = MF for DFE, LE, and an MF receiver, respectively. This allows us to formulate the FIR FF–BF filter optimization problem in a unified manner:

$$\max_{\boldsymbol{a}} \quad \mathrm{SINR}_{\mathrm{X}}(\boldsymbol{a}) \tag{49a}$$

$$\text{s.t.} \quad \boldsymbol{a}^H \boldsymbol{D}\boldsymbol{a} \leq P, \tag{49b}$$

where the power constraint (49b) is the same as in (14b). Although problem (49) formally looks very similar to problem (37), it is substantially more difficult to solve. The main reason for this lies in the fact that the optimization variable $\boldsymbol{a}(f)$ in (37) can be chosen freely for each frequency f, whereas the coefficient vector $\boldsymbol{a}$ in (49) is fixed for all frequencies. Fortunately, problem (49) has the same structure as the FIR FF–BF problem for single–antenna relays, and thus the efficient gradient algorithm provided in [5, Table 2] can be used to solve (49).

V. Simulation Results

In this section, we present simulation results for the SINR and the bit error rate (BER) of a cooperative network with FF–BF. Throughout this section we assume $\sigma_n^2 = \sigma_v^2 = 1$ and $P = 1$. This allows us to decompose the CIRs as $h_{i,z}[k] = \sqrt{\gamma_h}\,\bar{h}_{i,z}[k]$ and $g_{i,z}[k] = \sqrt{\gamma_g}\,\bar{g}_{i,z}[k]$, where γ_h and γ_g denote the transmitter signal–to–noise ratios (SNRs) of the relay–destination and the source–relay links, respectively. The normalized CIRs $\bar{h}_i[k]$ and $\bar{g}_i[k]$ include the effects of multipath fading and path–loss. All IIR and FIR FF–BF filters were obtained using the methods introduced in Sections III and IV.

The locations of the source, the destination, and the relays are shown in Fig. 2, where the numbers on top and beside the arrows indicate the normalized distance between the nodes. We consider the following three cooperative relay network setups: 1) $N_R = 1$ relays with $M_1 = 5$ at location (c); 2) $N_R = 2$ relays with $M_1 = 2$ and $M_2 = 3$ at locations (a) and (e), respectively; and 3) $N_R = 5$ relays with $M_z = 1$, $1 \leq z \leq N_R$, at locations (a)–(e), respectively. The normalized distance between the source and the destination is equal to 2 and the normalized horizontal distance between the source

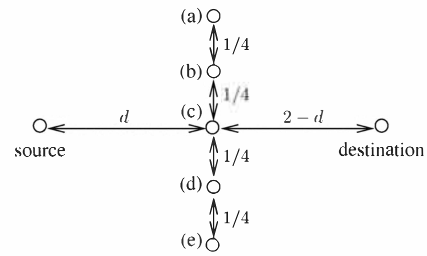

Fig. 2. Locations of source, destination, and relays in simulation.

and the relays is d. A path–loss exponent of 3 with reference distance $d_{\mathrm{ref}} = 1$ is assumed. The CIR coefficients of all links are modeled as independent quasi–static Rayleigh fading with $L_g = L_h = 5$ and following an exponential power delay profile $p[k] = \frac{1}{\sigma_t}\sum_{l=0}^{L_x-1} e^{-k/\sigma_t}\delta[k-l]$, where $L_x \in \{L_g, L_h\}$ and σ_t characterizes the delay spread [11]. All results shown were averaged over $100,000$ independent realizations of the fading channels.

A. FF–BF without Equalization

Figs. 3 and 4 show the average SINR vs. distance d for FF–BF for joint relay and joint source–relay power constraints, respectively. Relay network setups 1) – 3) were adopted. The FF–BF matrix filters were generated using the results in Section III-A and III-C, respectively. For both considered constraints FF–BF relaying enables considerable performance gains compared to direct transmission except for the case with $L_a = 1$, $N_R = 5$ and $M_z = 1$, $z \in \{1, 2, \ldots, 5\}$. Direct transmission is preferable only if the relay is located either closed to the source or the destination (small d or large d). The joint source–relay power constraint can yield significant performance gains if the relays are close to the source or close to the destination, respectively, by flexibly allocating more or less power to the source. Furthermore, Figs. 3 and 4 also show that it is preferable to have fewer relays with more antennas than more relays with fewer antennas.

Fig. 5 shows the total source and relay transmit power, $P_R + \sigma_s^2$, vs. the minimum required SINR γ at the destination for different relay network setups. The FF–BF matrix filters are generated based on the results in Sections III-B and III-D, respectively. Similar to [4], we have only included simulation points which guarantee feasibility of the optimization problem for more than 50 % of the channels. The total source and relay transmit power is computed by averaging over the feasible runs. The probability that this problem is feasible is shown in Fig. 6. From Figs. 5 and 6, we observe that joint source–relay transmit power minimization and multiple–antenna relays can lead to significant power savings. Fig. 5 also reveals that increasing L_a can substantially reduce the total source and relay transmit power.

B. FF–BF with Equalization

In Fig. 7, we show the average SINR vs. distance d for various FF–BF filter and equalization designs for relay nework setup 2) (i.e., $N_R = 2$, $M_1 = 2$, and $M_2 = 3$). We compare the performance of the proposed FF–BF matrix filter design with MMSE–DFE and without equalizer at the destination. Clearly, by adding a simple decision–feedback equalizer at the destination, performance gains of several dB can be achieved for all considered distances d. We note that for a given filter length L_a the feedback requirements and the relay complexity for the proposed FIR FF–BF schemes with or without equalization are identical. Fig. 7 also shows that as L_a increases, the

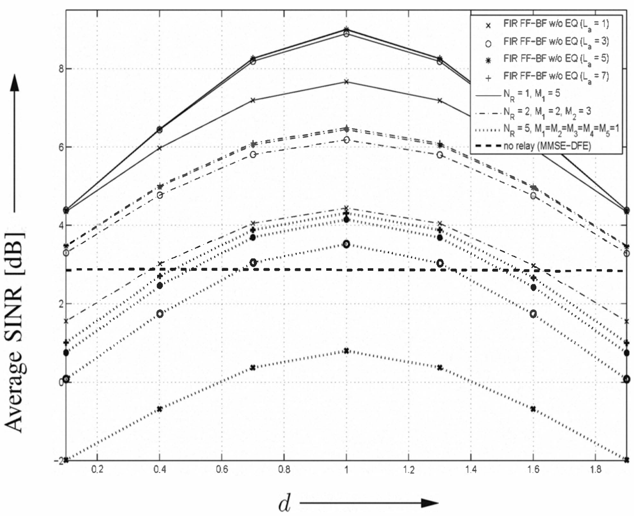

Fig. 3. Average SINR vs. distance d for FIR FF–BF without equalization (EQ) at the destination. The FF–BF matrix filters were optimized for a *joint relay power constraint.* Exponentially decaying channel power delay profile with $\sigma_t = 2$ and $L_g = L_h = 5$, and $\gamma_g = \gamma_h = 10$ dB. Results for direct transmission with transmit power $P = 2$ at the source are also included.

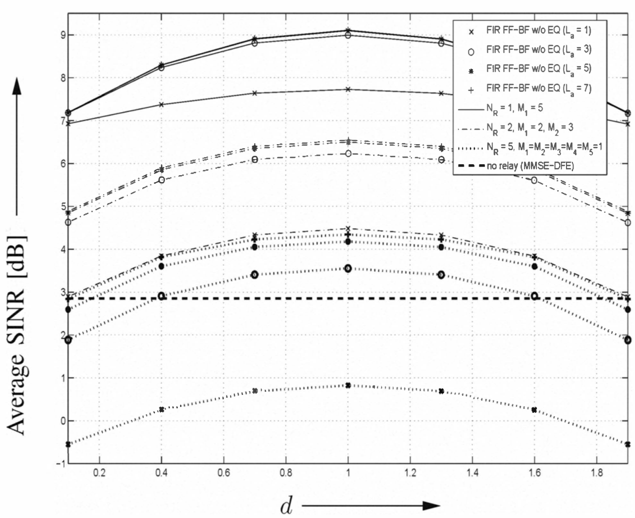

Fig. 4. Average SINR vs. distance d for FIR FF–BF without equalization (EQ) at the destination. The FF–BF matrix filters were optimized for a *joint source–relay power constraint.* Exponentially decaying channel power delay profile with $\sigma_t = 2$ and $L_g = L_h = 5$, and $\gamma_g = \gamma_h = 10$ dB. Results for direct transmission with transmit power $P = 2$ at the source are also included.

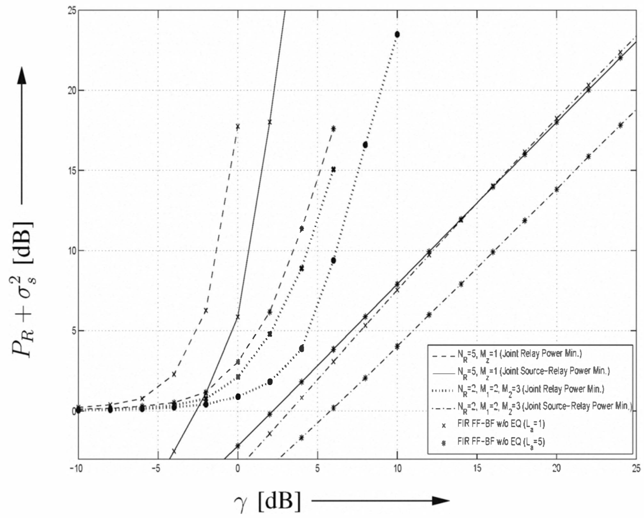

Fig. 5. Total average source and relay transmit power vs. required SINR γ for FIR FF–BF without equalization (EQ) at the destination for *relay power minimization* and *joint source–relay power minimization.* Exponentially decaying power delay profile with $\sigma_t = 2$ and $L_g = L_h = 5$, $d = 1$, and $\gamma_g = \gamma_h = 10$ dB.

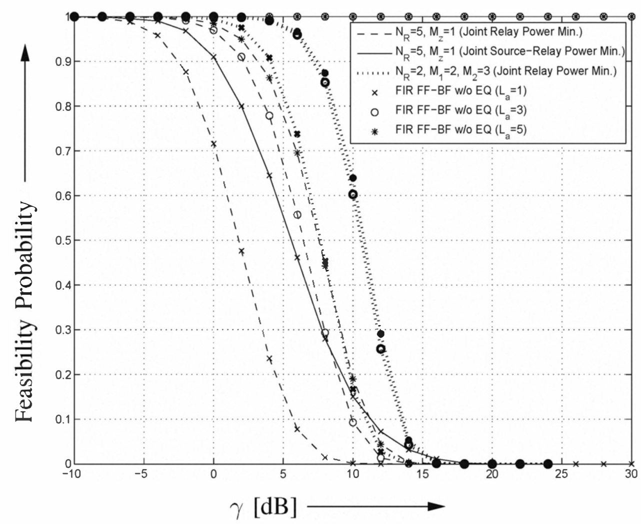

Fig. 6. Feasibility probability vs. required SINR γ for FIR FF–BF without equalization (EQ) at the destination for *relay power minimization* and *joint source–relay power minimization.* Exponentially decaying power delay profile with $\sigma_t = 2$ and $L_g = L_h = 5$, $d = 1$, and $\gamma_g = \gamma_h = 10$ dB.

performance of FIR FF–BF approaches the performance of IIR FF–BF with MMSE–DFE at the destination. For IIR FF–BF filters, Fig. 7 shows that the loss of MMSE–DFE compared to an idealized MF receiver, which is the ultimate performance bound for any equalizer architecture, exceeds 1 dB only for $d < 0.4$.

In Fig. 8, we investigate the impact of decay parameter σ_t on the performance of FF–BF for $d = 1$ and $\gamma_g = \gamma_h = 10$ dB. We note that the CIR coefficients of the test channel decay the faster (i.e., the channel is less frequency selective), the smaller σ_t is. As a special case, the channel becomes frequency flat when $\sigma_t = 0$. Fig. 8 shows that when the channel becomes frequency flat, i.e., $\sigma_t = 0$, all relaying schemes provide the same average SINR performance. We also observe that the performance of sufficiently long FF–BF filters is practically not affected by the frequency selectivity of the channel if MMSE–LE or MMSE–DFE are employed at the destination. The idealized MF receiver with IIR FF–BF benefits even slightly from more frequency selectivity (larger σ_t) because of the additional diversity offered by the channel. In contrast, FF–BF without equalization at the receiver is adversely affected by increased frequency selectivity and is even outperformed by direct transmission without relay (but with equalization at the destination) for $\sigma_t > 11$.

Fig. 9 shows BERs of BPSK modulation vs. transmit SNR, $\gamma = \gamma_g = \gamma_h$, for FIR and IIR FF–BF matrix filters. We adopt cooperative relay network setup 2), and assume $\sigma_t = 2$ and $d = 1$. The BERs for FIR FF–BF matrix filters were simulated by implementing MMSE–DFE with FIR equalization filters of lengths $4 \times L_{\text{eq}}$, which caused negligible performance degradation compared to IIR equalization filters. The BERs for IIR FF–BF were obtained by approximating the BER of BPSK transmission by $\text{BER}_{\text{X}} = Q(\sqrt{2\text{SINR}_{\text{X}}})$ [9], where

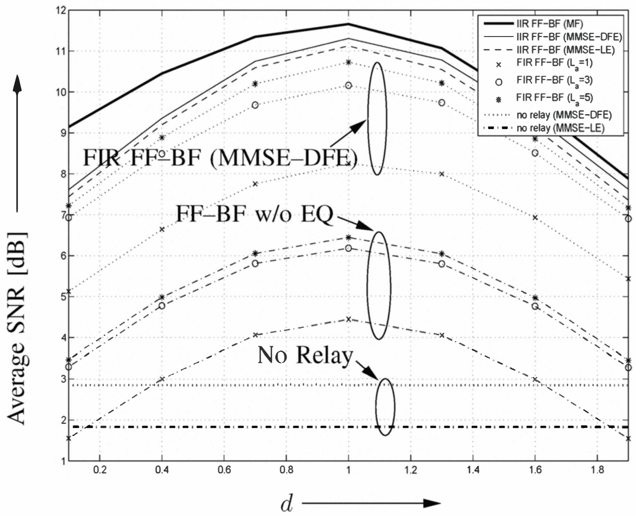

Fig. 7. Average SINR vs. distance d for FF–BF with MMSE–LE, MMSE–DFE, and an MF receiver at the destination. $N_R = 2$ relays with $M_1 = 2$ and $M_2 = 3$, exponentially decaying power delay profile with $\sigma_t = 2$ and $L_g = L_h = 5$, and $\gamma_g = \gamma_h = 10$ dB. For comparison the SINRs of FF–BF without (w/o) equalization (EQ) at the destination and without relaying are also shown, respectively.

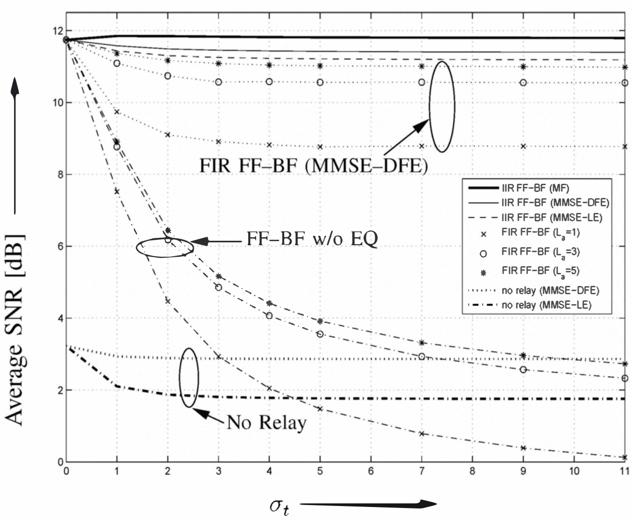

Fig. 8. Average SINR vs. decay parameter σ_t for FF–BF with MMSE–LE, MMSE–DFE, and an MF receiver at the destination. $N_R = 2$ relays with $M_1 = 2$ and $M_2 = 3$, distance $d = 1$, exponentially decaying power delay profile with $L_g = L_h = 5$, and $\gamma_g = \gamma_h = 10$ dB. For comparison the SINRs of FF–BF without (w/o) equalization (EQ) at the destination and without relaying are also shown, respectively.

X = DFE, X = LE, and X = MF for DFE, LE, and an MF receiver at the destination, respectively. Fig. 9 shows that equalization at the destination is very beneficial in terms of the achievable BER and large performance gains are realized compared to FF–BF without equalization. Also, for IIR FF–BF matrix filters MMSE–LE and MMSE–DFE receivers achieve practically identical BERs and the gap to the idealized MF receiver is less than 0.6 dB. This gap could potentially be closed by trellis–based equalizers, such as decision–feedback sequence estimation, at the expense of an increase in complexity.

VI. Conclusions

In this paper, we investigated FF–BF for relay networks with multiple multi–antenna relays and single–carrier transmission over frequency–selective channels. The FF–BF matrix filters at the relays were optimized for the cases where a simple slicer and LE/DFE were employed at the destination. For the first case, we can obtained closed–form solutions and efficient numerical methods for computation of the optimal FIR FF–BF matrix filters. For the second case, we obtained an elegant method for calculation of the optimal IIR FF–BF matrix filters and an efficient numerical algorithm for calculation of near–optimal FIR FF–BF matrix filters. Simulation results confirm that for a given total number of antennas it is preferable to have the antennas concentrated in few relays rather than having many relays with few antennas.

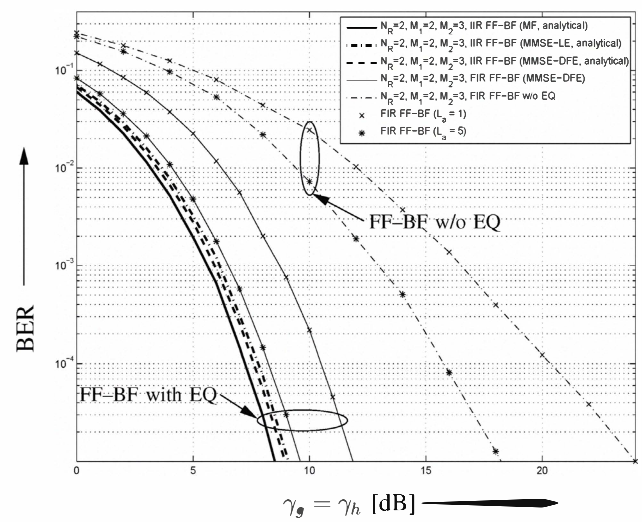

Fig. 9. Average BER of BPSK vs. transmit SNR γ for FF–BF with MMSE–LE, MMSE–DFE, and an MF receiver at the destination. Exponentially decaying power delay profile with $\sigma_t = 2$ and $L_g = L_h = 5$. For comparison the BER of FF–BF without (w/o) equalization (EQ) at the destination is also shown.

References

[1] R. Nabar, H. Bölcskei, and F. Kneubühler. Fading Relay Channels: Performance Limits and Space-Time Signal Design. *IEEE J. Select. Areas Commun.*, 22:1099–1109, August 2004.

[2] Y. Jing and H. Jafarkhani. Network Beamforming Using Relays With Perfect Channel Information. *IEEE Trans. Inform. Theory*, 55(6):2499–2517, June 2009.

[3] O. Munoz-Medina, J. Vidal, and A. Agustin. Linear Transceiver Design in Nonregenerative Relays With Channel State Information. *IEEE Trans. Signal Processing*, 55(6):2593–2604, June 2007.

[4] H. Chen, A. Gershman, and S. Shahbazpanahi. Filter-And-Forward Distributed Beamforming in Relay Networks with Frequency Selective Fading. *IEEE Trans. Signal Processing*, 58:1251–1262, March 2010.

[5] Y. Liang, A. Ikhlef, W. Gerstacker, and R. Schober. Cooperative Filter–and–Forward Beamforming for Frequency–Selective Channels with Equalization. Submitted to IEEE Trans. Wireless Commun., Available: http://www.ece.ubc.ca/~yangl/mimo_cap/TWC-10.pdf, 2010.

[6] J.G. Proakis. *Digital Communications.* McGraw–Hill, New York, forth edition, 2000.

[7] S. Boyd and L. Vandenberghe. *Convex Optimization.* Cambridge University Press, 2004.

[8] K.E. Baddour and P.J. McLane. Analysis of Optimum Diversity Combining and Decision Feedback Equalization in Dispersive Rayleigh Fading. In *Proc. of IEEE Intern. Commun. Conf.*, pages 21–26, June 1999.

[9] J. Cioffi, G. Dudevoir, M. Eyuboglu, and G. Forney Jr. MMSE Decision-Feedback Equalizers and Coding - Part I: Equalization Results. *IEEE Trans. Commun.*, 43:2582–2594, October 1995.

[10] J. Brewer. Kronecker Products and Matrix Calculus in System Theory. *IEEE Tran. on Circuits and Systems*, 25(9):772–781, September 1978.

[11] T. S. Rappaport. *Wireless Communications : Principles and Practice.* Prentice Hall, New York, 2002.